Use of TSAR, Thermal Shift Analysis in R, to identify Folic Acid as a Molecule that Interacts with HIV-1 Capsid

X. Gao[1,2,†], W. M. McFadden[1,2†], X. Wen[1,2], A. Emanuelli[1,2], Z. C. Lorson[1,2], H. Zheng[1,2], K. A. Kirby[1,2], S. G. Sarafianos[1,2,*]

[1]Center for ViroScience and Cure, Laboratory of Biochemical Pharmacology, Department of Pediatrics, Emory University School of Medicine, Atlanta, GA

[2]Children's Healthcare of Atlanta, Atlanta, GA

[†]These Authors contributed equally

*Correspondence (stefanos.sarafianos@emory.edu)

Abstract

Thermal shift assay (TSA) is a versatile biophysical technique for studying protein interactions. Here, we report a free, open-source software tool TSAR (Thermal Shift Analysis in R) to expedite and automate the analysis of thermal shift data derived either from individual experiments or large screens of chemical libraries. The TSAR package incorporates multiple, dynamic workflows to facilitate the analysis of TSA data and returns publication-ready graphics or processed results. Further, the package includes a graphic user interface (GUI) that enables easy use by non-programmers, aiming to simplify TSA analysis while diversifying visualization. To exemplify the utility of TSAR we screened a chemical library of vitamins to identify molecules that interact with the capsid protein (CA) of human immunodeficiency virus type 1 (HIV-1). Our data show that hexameric CA interacts with folic acid *in vitro*.

Introduction

The thermal shift assay (TSA), also called differential scanning fluorimetry (DSF), is an *in vitro* technique used to study the thermal stability of a purified protein or biological complex that has multiple applications [1-3]. During a TSA experiment, samples are heated to boiling temperatures at a constant rate to track the denaturation process of the protein(s) of interest. The denaturation of proteins that contain internal aromatic residues, like tryptophan, can be tracked without a dye by measuring the change in residue fluorescence [4]; however, TSA experiments often utilize a dye, like SYPRO™ Orange, to follow the exposure of the hydrophobic residues as denaturation progresses as the dye is fluorescent in hydrophobic environments [5]. Plotting the sample temperature compared to the fluorescence gives an individual melting profile for the protein or complex measured. The melting curve of an uncharacterized protein or complex can be

unpredictable, and testing of various dyes will help validate the findings [6]. For folded and globular proteins, hydrophobic residues are typically internal and inaccessible to the solvent, making TSA a useful tool to assess if a batch of proteins is properly folded, with low initial fluorescence readings, or denatured after purification, with high initial fluorescence readings near room temperature [7, 8].

For most samples that are properly folded, the thermal profile is sigmoidal, and a melting temperature (T_m) value can be calculated, representing the temperature where 50% of the protein is unfolded [2, 7]. The T_m is a useful value to compare the thermal stability of proteins under various conditions, such as choosing storage buffers and salts or for comparing the stability of mutant proteins [9, 10]. TSA is also useful for screening chemical libraries to identify potential binding partners for proteins, since protein•ligand interactions that form additional intramolecular bonds require more energy, or a higher temperature, to denature the sample compared to an unliganded protein [11, 12]. Thus, TSA has been used as a proxy readout for *in vitro* ligand binding within screens for protein inhibitors of a specific target.

This technique is used extensively in labs that focus on biological research, as it requires only a qPCR machine for data acquisition once a protein or biological complex is purified [2, 6]. The required volume and concentration of the sample are quite low, typically under 25 μL and below 20 μM per sample, although multiple replicates are needed when using TSA for comparison and analysis.

Present tools are Protein Thermal Shift™ Software v1.4 by Thermo Fisher Scientific (Waltham, MA), Serial Explorer in MATLAB, and open-source workflows provided through the Konstanz Information Miner (KNIME) [13]. While both tools from Thermo Fisher Scientific and MATLAB provide high-throughput analysis, they are proprietary and require additional costs.

Despite KNIME being open source, it offers only limited visualization options. Given the need to visualize the data in multiple dimensions and enhance accessibility of analysis tools we developed a software package written in R, a programming language extensively used for statistical and graphical analysis of biological data. 'TSAR', short for Thermal Shift Analysis in R, is a free and open-source software operating in R (version ≥ 4.3). It is distributed under an AGPL-3 license that offers a TSA analysis workflow as both command-line functions and an interactive ShinyR graphic user interface (GUI) dashboard [14, 15] (Figure 1). TSAR analysis incorporates either Boltzmann-fit or derivative-modeling of data to identify either T_m B (Boltzmann-fit) or T_m D (derivative-model) from melting curves with pipelines for easy comparisons of numerous dimensions, including T_ms, ligands, dosages, derivatives, and time series. The TSAR package is a complete suite of tools from initial data processing, T_m identification, automated data comparisons, and visualization of multiple publication-quality graphics for individual experiments to large screens with replicates (Figure 1B-E). TSAR is a well-documented package and has many custom settings for users experienced in R, while it also incorporates wrapping functions and a ShinyR dashboard to optionally minimize coding for easy use and quick implementation. Overall, TSAR aims to simplify TSA analysis yet diversify visualization.

Here, we perform an example TSA screen using the TSAR package to identify potential binding partners to the human immunodeficiency virus type 1 (HIV-1) capsid protein (CA). The HIV-1 capsid is an essential macromolecular structure within the mature viral core that serves as a reaction chamber for reverse transcription [16, 17]. It also protects the viral genome from cellular immune sensors as it traffics the genetic material to the nucleus [18, 19]. As it is important in numerous steps throughout the HIV-1 replication cycle, investigating the biology of the capsid core is of great importance in the design of next-generation antiretroviral therapies (ART) [18]. In

fact, when the CA-targeting compound Lenacapavir (also called Sunlenca® or GS-6207) was approved for use in highly-treatment experienced patients in 2022, CA became the first new target for a clinically used ART class in over a decade [20, 21]. CA is a great clinical target, as it is a highly conserved and genetically fragile protein; the kinetics of CA•CA interactions are finely tuned for balancing cellular trafficking and genome release, such that both increasing and decreasing capsid stability has a negative impact on viral fitness [9, 18, 22-25]. Recent reports have demonstrated that CA interacts with inositol hexaphosphate (IP6) and deoxyribonucleotides (dNTPs) to regulate and increase capsid stability [26-28]. As there are reports that HIV-1 infection modulates cellular metabolism, both in the presence and absence of ART, we hypothesized that there might be additional endogenous interactions with other common protein cofactors [29, 30]. Thus, we screened a library of essential vitamins (Sigma, St Louis, MO) for interactions with a disulfide-stabilized HIV-1 capsid hexamer and found that folic acid shifted the T_m D by 3.04°C. This screen provides an example workflow for the TSAR R package, a tool that can be broadly used in protein biology.

Methods

Distribution and Package Information

TSAR (Thermal Shift Analysis in R) is an open-source package written in R (≥4.3) [15]. It is freely distributed under an AGPL-3 license in the Bioconductor R package repository (V ≥3.18) [31] at https://bioconductor.org/packages/TSAR. A prerequisite for downloading TSAR through R requires that the BiocManager R package [32] be installed prior; installing TSAR is accomplished with the following line of code: *BiocManager::install("TSAR")*. TSAR was coded and documented using

RStudio GUI [33] and the devtools package [34]. TSAR contains well-documented functions and three vignettes (long-form documentation) to assist users. TSAR depends on tidyverse packages [35] as well as: jsonlite [36], openxlsx [37], mgcv [38-40], and minpack.lm [41] packages for analysis, and shiny [14], shinyWidgets [42], plotly [43], shinyjs [44], rhandsontable [45], and ggpubr [46] packages for the Shiny R GUI and data visualizations.

Package Structure

TSAR is sectioned into three individual operating dashboards, Data Preprocessing, Data Analysis, and Data Visualization, each with one command line call (Figure 1B). While users may conduct all procedures and analyses within the established GUI, this package also allows command-line approaches where users may implement more options and flexibilities with their analysis. Mathematical modeling in TSAR relies on both generalized additive models and non-linear modeling to compute T_m D and T_m B values.

TSAR allows visualization of data on multiple dimensions, taking T_m (50% protein unfolding temperature) analysis further, providing a comparison of numerous dimensions, including aspects of, but not limited to T_ms, ligands, dosages, derivatives, and time series.

Statistics and Analysis

TSAs result in a standard curve characterized by initial low fluorescence, an increasing peak, and trailing fluorescence slowly decreasing back to the initial level. To study such peaks, mathematical modeling is required (Figure 2A). Combining with machine learning, TSAR utilizes the generalized additive model from mgcv package to capture the derivatives of the curve and the inflection point, T_m D [38-40]. Meanwhile, TSAR utilizes non-linear modeling from the

minpack.lm package [41] in R to capture Boltzmann curves with machine-learned minimum and maximum. By this mechanism, TSAR is able to characterize the fluorescence trend in Boltzmann fit fashion, locating the T_m B. Both methods may switch between easily within the GUI and command line. To assess the accuracy of TSAR, we benchmarked its calculations of T_m and ΔT_m shift to those of Protein Thermal Shift Software V1.4 (Thermo Fisher Scientific). Setting Protein Thermal Shift Software calculations as the baseline literature value, the error of TSAR T_m D is centered at 0.048 with a variance of 0.063 degree Celsius (Supplementary Figure S1A). Meanwhile, the error of TSAR T_m B is centered at 1.029 with a variance of 0.634 degree Celsius (Supplementary Figure S1B). While that error is relatively greater than T_m D, the error is systematic where computing ΔT_m B by using DMSO as the baseline control yield errors centering at 0.376 °C (Supplementary Figure S1C-D).

Testing the library yielded significant result for the folic acid with ΔT_m D shift of 3.04 °C. Testing at 50 μM, 25 μM, and 7.5 μM compound, the first derivative comparison graphs demonstrate that the ΔT_m of folic acid with CA121 is dose dependent (Figure 3). At 7.5 μM, protein unfolding curves are distinguishable from DMSO control, but ΔT_m experiences greater variance. Conducting one-tailed, paired T tests show that all treatment conditions are significantly different from the DMSO control, with 50 μM and 25 μM folic acid significant at the level of 5E-5, and 7.5 μM folic acid significant at the level of 5E-3 (Figure 3D).

Protein Purification

The CA hexamers with A14C/E45C/W184A/M185A mutations (CA121) were cloned into a pET11a expression plasmid, which was provided by Dr. Owen Pornillos from the University of Virginia. The expression and purification of CA121 were carried out in *E. coli* BL21(DE3)RIL as

previously described [47]. Additionally, full-length, wild-type CA monomers (CA FL) were cloned into a pET11a expression plasmid, provided by Dr. Chun Tang from Peking University. The expression of CA FL was performed in *E. coli* BL21(DE3)RIL and purification involved ammonium sulfate precipitation followed by anion exchange chromatography, as previously described [25].

Compounds

Library chemicals were purchased as part of the Vitamins Kit (Sigma Aldrich, V1-1KT) and resuspended in DMSO to a final concentration of 10-50 mM and stored at -20°C. Compounds included: D-Pantothenic acid hemicalcium salt (B5), Biotin, Nicotinamide (B3), 4-Aminobenzoic acid (4-ABA), Pyridoxamine dihydrochloride (PyxAmine diHCl), Pyridoxine hydrochloride (PyxINE HCl), Thiamine hydrochloride (Thiamine HCl), Folic Acid (B9), (±)-α-Lipoic acid (a-LA), Pyridoxal hydrochloride (Pyxal HCl). 50% Phytic acid solution (Sigma Aldrich) was used as the IP6 positive controls.

Thermal Shift Assay (TSA)

TSAs were conducted using QuantStudio 3 Real-Time PCR Systems (Thermo Fisher Scientific, Waltham, MA) with a final reaction volume of 20 µL and ≤1% DMSO. The sample fluorescence was measured while being heated from 25–95°C at a constant rate of 0.2°C/10s, consistent with the methodology outlined in previous studies [6, 9, 11]. Proteins were tested at a final concentration of 7.5 µM in a 50 mM Tris (pH 8.0) and supplemented with 1x SYPRO™ Orange Protein Gel Stain (Life Technologies) after incubation with the compounds for 30 minutes on ice. In the initial screening of the library, the CA121 protein (7.5 µM) was incubated with 25 µM of each compound. Fluorescence intensity for each sample was measured as described, and thermal profiles were assessed using TSAR or Protein Thermal Shift Software v1.3 (Applied

Biosystems) (Figure 2B-C). The compounds that induced a shift in the T_m (ΔT_m) at 25 µM underwent further testing in a dose-response manner under concentrations of 7.5 µM and 50 µM (Figure 3).

Lastly, all compounds leading to significant thermal shifts were also tested in the presence of the tris(2-carboxyethyl)phosphine (TCEP)-reducing agent. TCEP functions to break the CA121 disulfide stabilizing bonds, possibly affecting the stability of pockets formed by multiple CA monomers [26]. Comparing the fluorescence profile of TSA samples with and without TCEP provides insight into the potential interactions of a compound with the monomer versus the hexamer CA protein (Figure 4).

Discussion

Here, we performed a screen of protein•ligand interactions by conducting a thermal shift assay (TSA) and analyzed the results with the open-source R package, TSAR. We found that the HIV-1 capsid protein hexamers interact with folic acid *in vitro*. TSAR is a novel package for the R coding language, which has become a common tool taught in higher-education coursework and used by many biological research labs. There are other software tools for TSA data analysis, like the proprietary software offered by Thermo Fisher Scientific or open-source packages offered for the proprietary MATLAB software. However, these typically have some cost associated with implementing or installing the software. TSAR is written in the R coding language, which is free, and distributed under an AGPL license, ensuring there is no cost for analyzing the data.

There are reports identifying endogenous metabolites as important cofactors in HIV-1 replication that interact specifically with mature capsid hexamers [47], including IP6 that is

important for capsid assembly and stability as well as dNTPs that are needed for reverse transcription and genome replication [16-19, 26, 27]. This study does not establish the biological significance of folic acid for the replication cycle of HIV-1. Of note, many individuals living with HIV-1 have a deficiency in folic acid metabolism [48, 49], though it is not clear these findings are related. Folic acid is an important factor required for cell growth and development; folic acid deficiency can lead to neuronal defects and anemia [50, 51]. Thus, it is of interest that this critical cellular metabolite may interact with and stabilize HIV-1 capsid hexamers. The role and relevance of folic acid in HIV-1 biology remains a topic of investigation, but the findings of the screen reported here indicate the ability for assembled hexamers, but not unassembled monomeric capsid, to interact with folic acid.

Acknowledgments

This research was supported in part by the National Institutes of Health (R01 AI120860, P30 AI050409, U54 AI170855, to SGS; WMM was supported in part by T32 GM135060 and F31 AI174951). The content is solely the responsibility of the authors and does not necessarily represent the official views of the National Institutes of Health. SGS acknowledges funding from the Nahmias-Schinazi Distinguished Chair in Research. For providing essential details in making the package, we would like to acknowledge the book R Packages by Hadley Wickham (O'Reilly) ©2015 Hadley Wickham, ISBN: 978-1-491-91059-7.

Author contributions

Conceptualization, WMM, KAK, and SGS; Methodology & Investigation, XG, WMM, XW, HZ, AE, and ZCL; Resources, WMM, KAK, AE, and ZCL; Visualization, XG and WMM; Writing –

Original Draft, XG, WMM and SGS; Writing – Review & Editing, XG, WMM, SGS; Supervision, WMM, KAK, and SGS; Funding Acquisition, WMM, KAK and SGS.

Declaration of interests

The authors declare no competing interests.

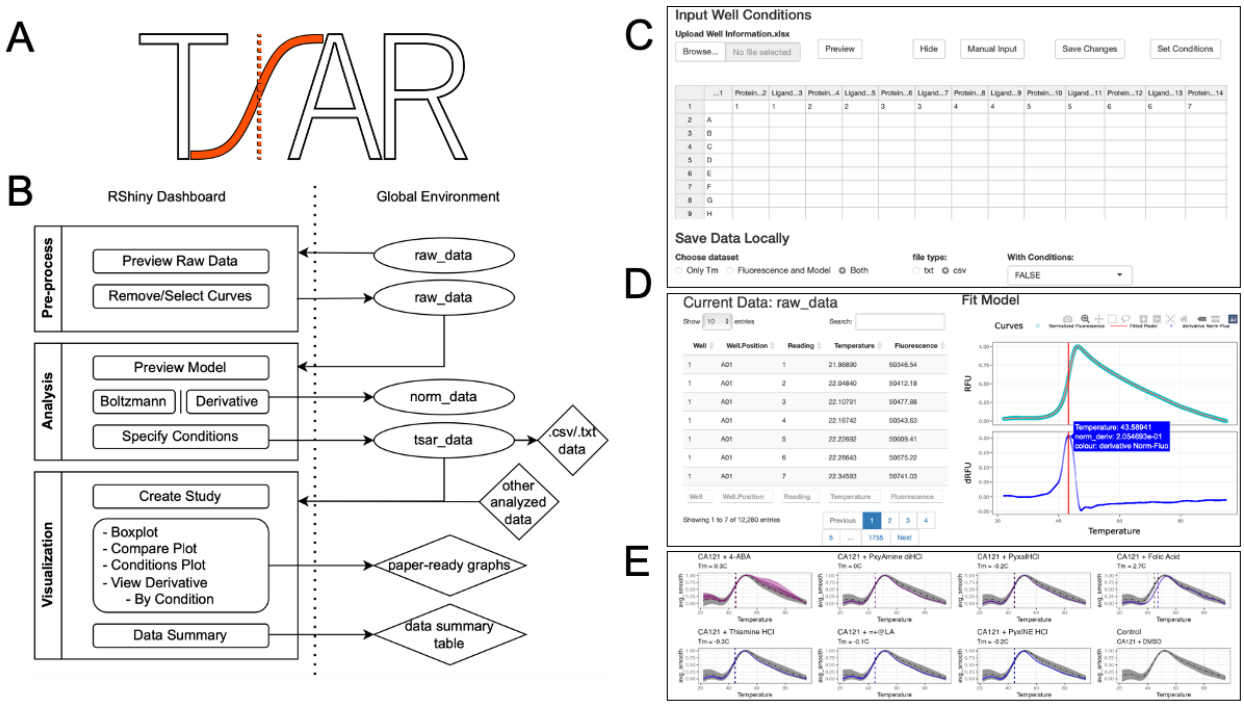

Figure 1 – A) TSAR Logo. B) Workflow for TSAR, supporting data import and export at various stages. C-E) Screenshots of the TSAR program. C) shows the Shiny R GUI for importing data. D) shows the interactive data analysis that TSAR performs, E) is an example of a partial output from a library screen.

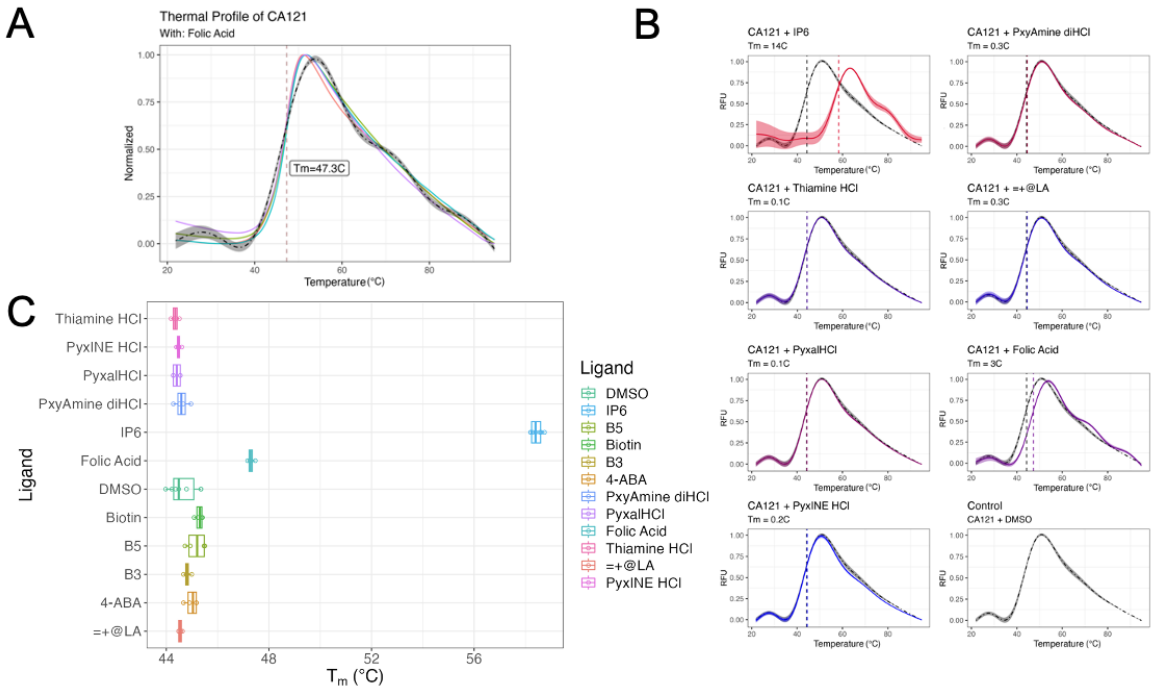

Figure 2 – A) Compare plot further showcases the interaction curves. Graphed as RFU (relative fluorescence unit) over Temperature (degree Celsius) in color as contrast to DMSO control in grey. Only IP6, positive control, and Folic Acid yields significant T_m change. IP6: ΔT_m D = 13.75°C at significance level < 5E-11. Folic Acid: ΔTm D = 3.04°C at significance level < 5E-5. B) Folic Acid thermal shift assay profiles by individual sample (n = 4). Each individual trial is mapped in a differently colored curve. Graph shows normalized RFU (relative fluorescence unit) as y-axis. Alternate options are allowed in TSAR package. The grey line represents average between all samples of a condition. C) Screening all vitamin compounds at 50 µM with CA121 hexamer protein at 7.5 µM. All compounds were suspended in DMSO, thus compared to negative control, DMSO. Initial screening shows that folic acid shows a 3.04°C of Tm D shift, indicating interactions with CA121 while it unfolds.

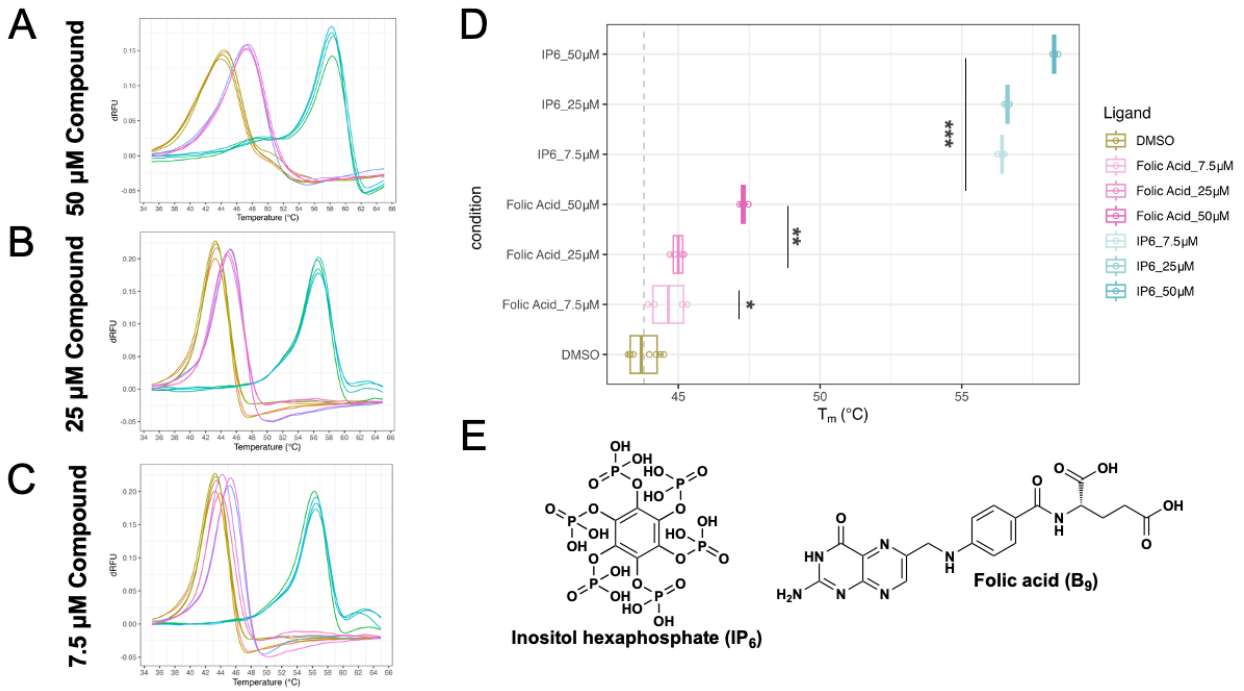

Figure 3. Dose dependence study of folic acid and CA121 shows ΔT_m is dosage-dependent yet still significant. A-C) First derivative comparison graphs demonstrate that ΔT_m of folic acid with CA121 is dose dependent at A) 50 µM, B) 25 µM, C) 7.5 µM compound. At 7.5 µM, protein unfolding curves are distinguishable, but suffers greater variance. D) Each condition (n = 4) consist of ligand suspended in DMSO and CA121 hexamer protein in Tris buffer at pH 8.0. IP6 is diluted in Tris directly without DMSO. One-tailed t-tests show that all treatment conditions are significantly different from the DMSO control. * indicates significance at 5E-3, ** indicates significance at 5E-5, and *** indicates significance at 5E-9 E) Chemical Structures of hits, Folic Acid and IP6. Made in ChemDraw V19.0.

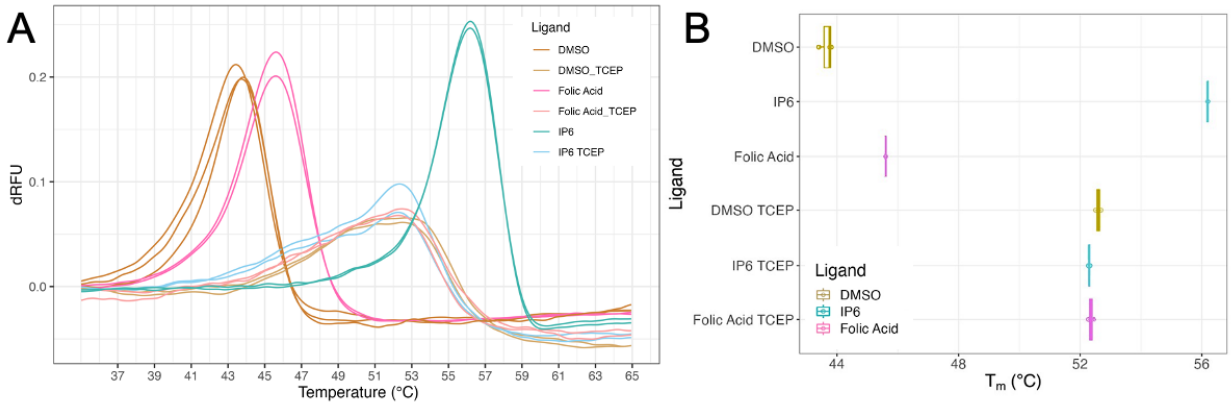

Figure 4. Reducing CA121 shows Thermal Shift in folic acid is protein specific. TCEP was added as a reducing agent to break apart CA121, eliminating the central pore of protein-ligand interaction. A) TSA performed with ligands at 25 µM. Comparing first derivatives show that TCEP alters regular protein fluorescence curve. B) Boxplot demonstrates adding TCEP leads to insignificant ΔT_m D.

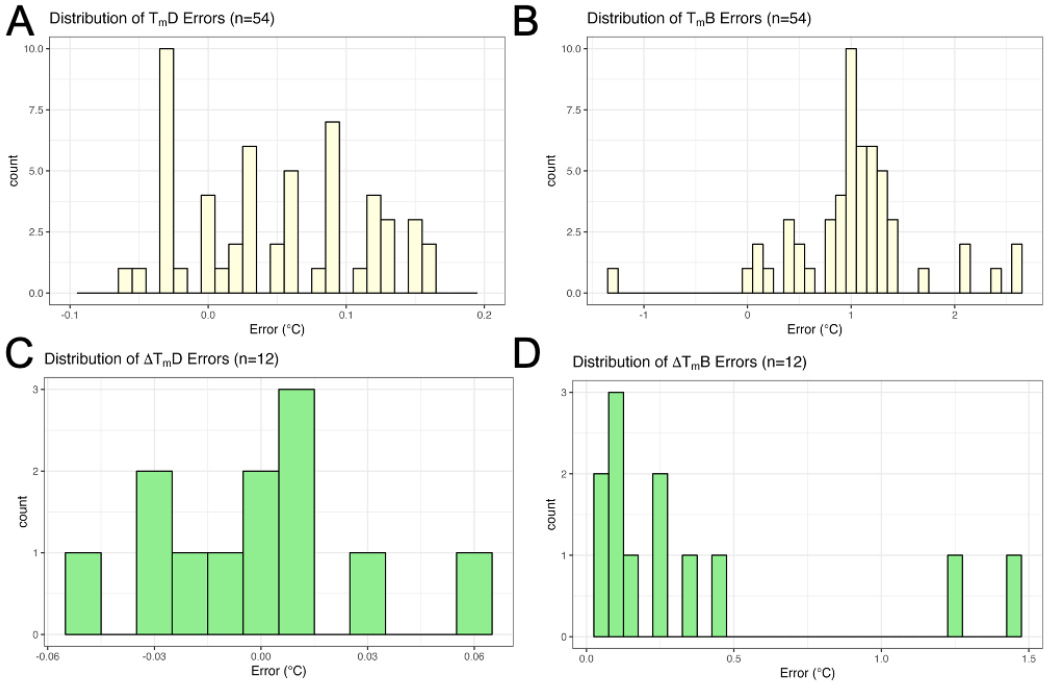

Supplementary Figure 1. TSAR accuracy compared to Protein Thermal Shift™. A, C) Derivative estimation errors. (n = 54) is N~(0.048, 0.063). ΔT_m D estimation error is similarly distributed, N~(-0.001, 0.029). **B, D)** Boltzmann estimation errors (n = 54) is approximately N~(1.029, 0.634). ΔT_m B estimation error is biased in the positive direction, N~(0.376, 0.451).

References

1. Andreotti G, Monticelli M, Cubellis MV. Looking for protein stabilizing drugs with thermal shift assay. Drug Testing and Analysis. 2015;7(9):831-4. doi: https://doi.org/10.1002/dta.1798.

2. Gao K, Oerlemans R, Groves MR. Theory and applications of differential scanning fluorimetry in early-stage drug discovery. Biophys Rev. 2020;12(1):85-104. Epub 2020/02/02. doi: 10.1007/s12551-020-00619-2. PubMed PMID: 32006251; PubMed Central PMCID: PMCPMC7040159.

3. Huynh K, Partch CL. Analysis of Protein Stability and Ligand Interactions by Thermal Shift Assay. Current Protocols in Protein Science. 2015;79(1):28.9.1-.9.14. doi: https://doi.org/10.1002/0471140864.ps2809s79.

4. Magnusson AO, Szekrenyi A, Joosten H-J, Finnigan J, Charnock S, Fessner W-D. nanoDSF as screening tool for enzyme libraries and biotechnology development. The FEBS Journal. 2019;286(1):184-204. doi: https://doi.org/10.1111/febs.14696.

5. Lo M-C, Aulabaugh A, Jin G, Cowling R, Bard J, Malamas M, et al. Evaluation of fluorescence-based thermal shift assays for hit identification in drug discovery. Analytical Biochemistry. 2004;332(1):153-9. doi: https://doi.org/10.1016/j.ab.2004.04.031.

6. Niesen FH, Berglund H, Vedadi M. The use of differential scanning fluorimetry to detect ligand interactions that promote protein stability. Nature Protocols. 2007;2(9):2212-21. doi: 10.1038/nprot.2007.321.

7. Wu T, Hornsby M, Zhu L, Yu JC, Shokat KM, Gestwicki JE. Protocol for performing and optimizing differential scanning fluorimetry experiments. STAR protocols. 2023;4(4):102688.

8. Biter AB, de la Peña AH, Thapar R, Lin JZ, Phillips KJ. DSF Guided Refolding As A Novel Method Of Protein Production. Scientific Reports. 2016;6(1):18906. doi: 10.1038/srep18906.

9. Miyazaki Y, Doi N, Koma T, Adachi A, Nomaguchi M. Novel In Vitro Screening System Based on Differential Scanning Fluorimetry to Search for Small Molecules against the Disassembly or Assembly of HIV-1 Capsid Protein. Front Microbiol. 2017;8(1413):1413. Epub 2017/08/10. doi: 10.3389/fmicb.2017.01413. PubMed PMID: 28791001; PubMed Central PMCID: PMCPMC5522879.

10. Layton CJ, Hellinga HW. Quantitation of protein–protein interactions by thermal stability shift analysis. Protein Science. 2011;20(8):1439-50. doi: https://doi.org/10.1002/pro.674.

11. Vernekar SKV, Sahani RL, Casey MC, Kankanala J, Wang L, Kirby KA, et al. Toward Structurally Novel and Metabolically Stable HIV-1 Capsid-Targeting Small Molecules. Viruses. 2020;12(4):452. PubMed PMID: doi:10.3390/v12040452.

12. Krishna SN, Luan C-H, Mishra RK, Xu L, Scheidt KA, Anderson WF, et al. A Fluorescence-Based Thermal Shift Assay Identifies Inhibitors of Mitogen Activated Protein Kinase Kinase 4. PLOS ONE. 2013;8(12):e81504. doi: 10.1371/journal.pone.0081504.

13. Samuel ELG, Holmes SL, Young DW. Processing binding data using an open-source workflow. Journal of Cheminformatics. 2021;13(1):99. doi: 10.1186/s13321-021-00577-1.

14. Chang W, Cheng J, Allaire J, Xie Y, McPherson J, Dipert A, et al. shiny: Web Application Framework for R. 2023.

15. R Core Team. R: A language and environment for statistical computing. 4.3.1 ed. Vienna, Austria: R Foundation for Statistical Computing, ; 2023.

16. Aiken C, Rousso I. The HIV-1 capsid and reverse transcription. Retrovirology. 2021;18(1):29. doi: 10.1186/s12977-021-00566-0.

17. Campbell EM, Hope TJ. HIV-1 capsid: the multifaceted key player in HIV-1 infection. Nat Rev Microbiol. 2015;13(8):471-83. Epub 2015/07/17. doi: 10.1038/nrmicro3503. PubMed PMID: 26179359; PubMed Central PMCID: PMCPMC4876022.

18. McFadden WM, Snyder AA, Kirby KA, Tedbury PR, Raj M, Wang Z, et al. Rotten to the core: antivirals targeting the HIV-1 capsid core. Retrovirology. 2021;18(1):41. doi: 10.1186/s12977-021-00583-z.

19. Müller TG, Zila V, Müller B, Kräusslich H-G. Nuclear Capsid Uncoating and Reverse Transcription of HIV-1. Annual Review of Virology. 2022;9(1):261-84. doi: 10.1146/annurev-virology-020922-110929.

20. Dvory-Sobol H, Shaik N, Callebaut C, Rhee MS. Lenacapavir: a first-in-class HIV-1 capsid inhibitor. Current Opinion in HIV and AIDS. 2022;17(1):15-21.

21. McFadden WM, Sarafianos SG. Targeting the HIV-1 and HBV Capsids, an EnCore. Viruses. 2023;15(4):896. PubMed PMID: doi:10.3390/v15040896.

22. Lamorte L, Titolo S, Lemke CT, Goudreau N, Mercier JF, Wardrop E, et al. Discovery of novel small-molecule HIV-1 replication inhibitors that stabilize capsid complexes. Antimicrob Agents Chemother. 2013;57(10):4622-31. Epub 2013/07/03. doi: 10.1128/AAC.00985-13. PubMed PMID: 23817385; PubMed Central PMCID: PMCPMC3811413.

23. Rihn SJ, Wilson SJ, Loman NJ, Alim M, Bakker SE, Bhella D, et al. Extreme Genetic Fragility of the HIV-1 Capsid. PLOS Pathogens. 2013;9(6):e1003461. doi: 10.1371/journal.ppat.1003461.

24. Blair WS, Pickford C, Irving SL, Brown DG, Anderson M, Bazin R, et al. HIV capsid is a tractable target for small molecule therapeutic intervention. PLoS Pathog. 2010;6(12):e1001220. Epub 2010/12/21. doi: 10.1371/journal.ppat.1001220. PubMed PMID: 21170360; PubMed Central PMCID: PMCPMC3000358.

25. Gres AT, Kirby KA, KewalRamani VN, Tanner JJ, Pornillos O, Sarafianos SG. X-ray crystal structures of native HIV-1 capsid protein reveal conformational variability. Science. 2015;349(6243):99-103. Epub 2015/06/06. doi: 10.1126/science.aaa5936. PubMed PMID: 26044298; PubMed Central PMCID: PMCPMC4584149.

26. Jacques DA, McEwan WA, Hilditch L, Price AJ, Towers GJ, James LC. HIV-1 uses dynamic capsid pores to import nucleotides and fuel encapsidated DNA synthesis. Nature. 2016;536(7616):349-53. doi: 10.1038/nature19098.

27. Dick RA, Zadrozny KK, Xu C, Schur FKM, Lyddon TD, Ricana CL, et al. Inositol phosphates are assembly co-factors for HIV-1. Nature. 2018;560(7719):509-12. doi: 10.1038/s41586-018-0396-4.

28. Renner N, Mallery DL, Faysal KMR, Peng W, Jacques DA, Böcking T, et al. A lysine ring in HIV capsid pores coordinates IP6 to drive mature capsid assembly. PLOS Pathogens. 2021;17(2):e1009164. doi: 10.1371/journal.ppat.1009164.

29. Castellano P, Prevedel L, Valdebenito S, Eugenin EA. HIV infection and latency induce a unique metabolic signature in human macrophages. Scientific Reports. 2019;9(1):3941. doi: 10.1038/s41598-019-39898-5.

30. Clerc I, Abba Moussa D, Vahlas Z, Tardito S, Oburoglu L, Hope TJ, et al. Entry of glucose- and glutamine-derived carbons into the citric acid cycle supports early steps of HIV-1 infection in CD4 T cells. Nature Metabolism. 2019;1(7):717-30. doi: 10.1038/s42255-019-0084-1.

31. Gentleman RC, Carey VJ, Bates DM, Bolstad B, Dettling M, Dudoit S, et al. Bioconductor: open software development for computational biology and bioinformatics. Genome Biology. 2004;5(10):R80. doi: 10.1186/gb-2004-5-10-r80.

32. Morgan M, Ramos M. BiocManager: Access the Bioconductor Project Package Repository. p. R package version 1.30.22.

33. Posit team. RStudio: Integrated Development Environment for R. 2023.

34. Wickham H, Hester J, Chang W, J B. devtools: Tools to Make Developing R Packages Easier. 2022.

35. Wickham H, Averick M, Bryan J, Chang W, McGowan LDA, François R, et al. Welcome to the Tidyverse. Journal of open source software. 2019;4(43):1686.

36. Ooms J. The jsonlite Package: A Practical and Consistent Mapping Between JSON Data and R Objects. arXiv:1403 2805 [stat CO]. 2014.

37. Schauberger P, Walker A. openxlsx: Read, Write and Edit xlsx Files. 2023.

38. Wood SN. Fast stable restricted maximum likelihood and marginal likelihood estimation of semiparametric generalized linear models. Journal of the Royal Statistical Society (B). 2011;73(1):3-36.

39. Wood SN, Pya N, Saefken B. Smoothing parameter and model selection for general smooth models (with discussion). Journal of the American Statistical Association. 2016;111:1548-75.

40. Wood SN. Generalized Additive Models: An Introduction with R. 2017. Epub 2.

41. Elzhov TV, Mullen KM, Spiess A-N, Bolker B. minpack.lm: R Interface to the Levenberg-Marquardt Nonlinear Least-Squares Algorithm Found in MINPACK, Plus Support for Bounds. 2023.

42. Perrier V, Meyer F, Granjon D. shinyWidgets: Custom Inputs Widgets for Shiny. 2023.

43. Sievert C. Interactive Web-Based Data Visualization with R, plotly, and shiny. 2020.

44. Attali D. shinyjs: Easily Improve the User Experience of Your Shiny Apps in Seconds. 2021.

45. Owen J. rhandsontable: Interface to the 'Handsontable.js' Library. 2021.

46. Kassambara A. ggpubr: 'ggplot2' Based Publication Ready Plots. R package version 0.6.0 ed2023. p. R package version 0.6.0}.

47. Pornillos O, Ganser-Pornillos BK, Kelly BN, Hua Y, Whitby FG, Stout CD, et al. X-ray structures of the hexameric building block of the HIV capsid. Cell. 2009;137(7):1282-92. Epub 2009/06/16. doi: 10.1016/j.cell.2009.04.063. PubMed PMID: 19523676; PubMed Central PMCID: PMCPMC2840706.

48. Adhikari PM, Chowta MN, Ramapuram JT, Rao S, Udupa K, Acharya SD. Prevalence of Vitamin B(12) and folic acid deficiency in HIV-positive patients and its association with neuropsychiatric symptoms and immunological response. Indian J Sex Transm Dis AIDS. 2016;37(2):178-84. Epub 2016/11/29. doi: 10.4103/0253-7184.192117. PubMed PMID: 27890954; PubMed Central PMCID: PMCPMC5111305.

49. Revell P, O'Doherty MJ, Tang A, Savidge GF. Folic acid absorption in patients infected with the human immunodeficiency virus. Journal of Internal Medicine. 1991;230(3):227-31. doi: https://doi.org/10.1111/j.1365-2796.1991.tb00435.x.

50. Donnelly JG. Folic Acid. Critical Reviews in Clinical Laboratory Sciences. 2001;38(3):183-223. doi: 10.1080/20014091084209.

51. Mahmood L. The metabolic processes of folic acid and Vitamin B12 deficiency. Journal of Health Research and Reviews (In Developing Countries). 2014;1(1):5-9.

A

TSAR

B

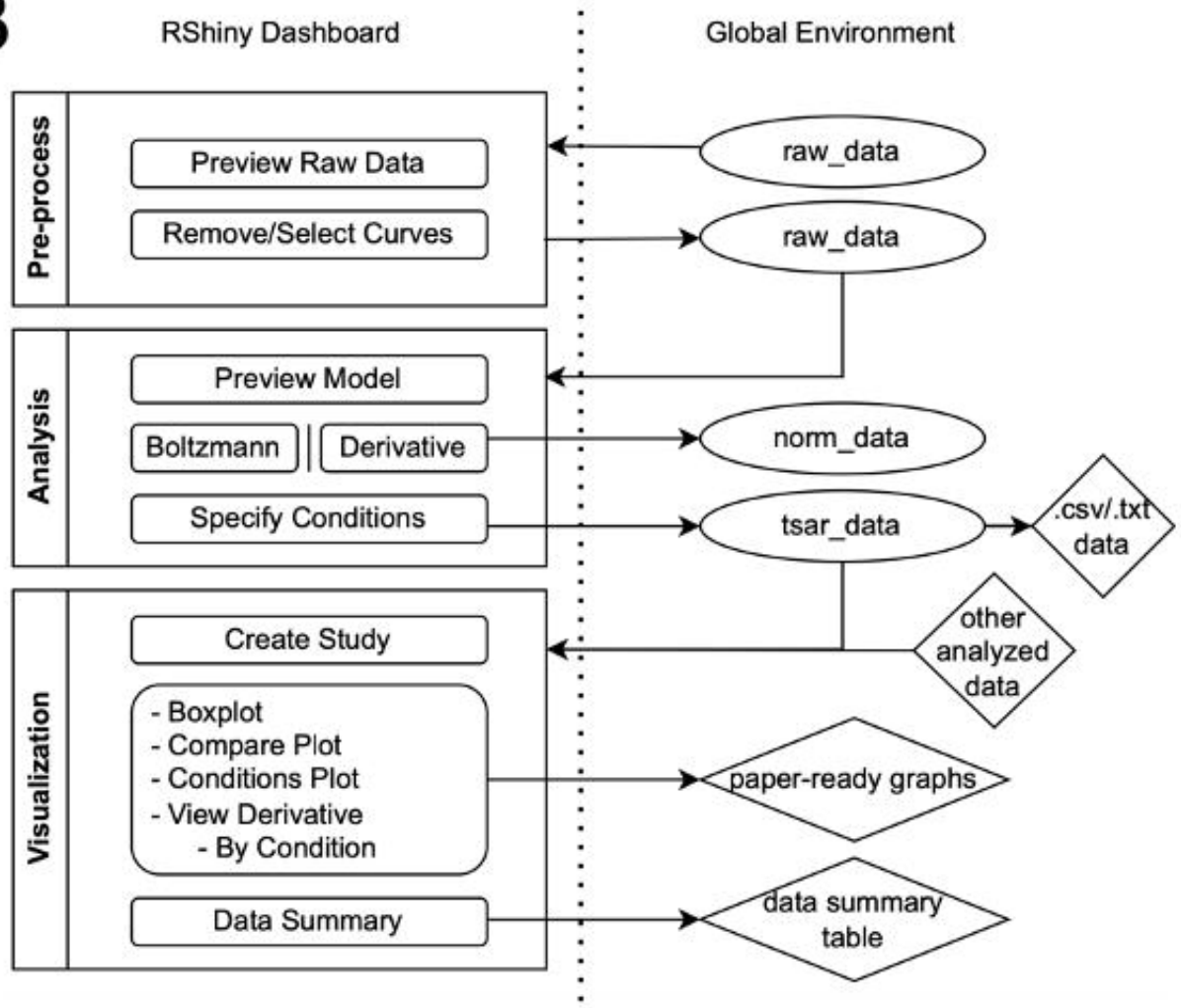
RShiny Dashboard
Global Environment
Pre-process
Preview Raw Data
Remove/Select Curves
raw_data
raw_data
Analysis
Preview Model
Boltzmann
Derivative
Specify Conditions
norm_data
tsar_data
.csv/.txt data
other analyzed data
Visualization
Create Study
- Boxplot
- Compare Plot
- Conditions Plot
- View Derivative
- By Condition
Data Summary
paper-ready graphs
data summary table

C

Input Well Conditions
Upload Well Information.xlsx
Browse...
No file selected
Preview
Hide
Manual Input
Save Changes
Set Conditions
Save Data Locally
Choose dataset
Only Tm
Fluorescence and Model
Both
file type:
txt
csv
With Conditions:
FALSE

D

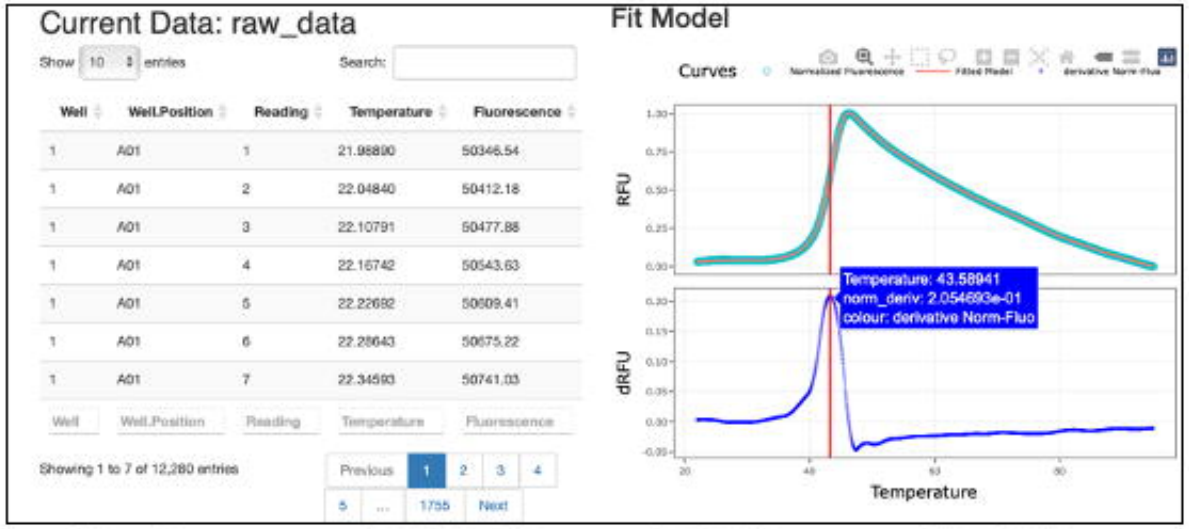
Current Data: raw_data
Fit Model
Curves
RFU
dRFU
Temperature
Temperature: 43.58941
norm_deriv: 2.054693e-01
colour: derivative Norm-Fluo

E

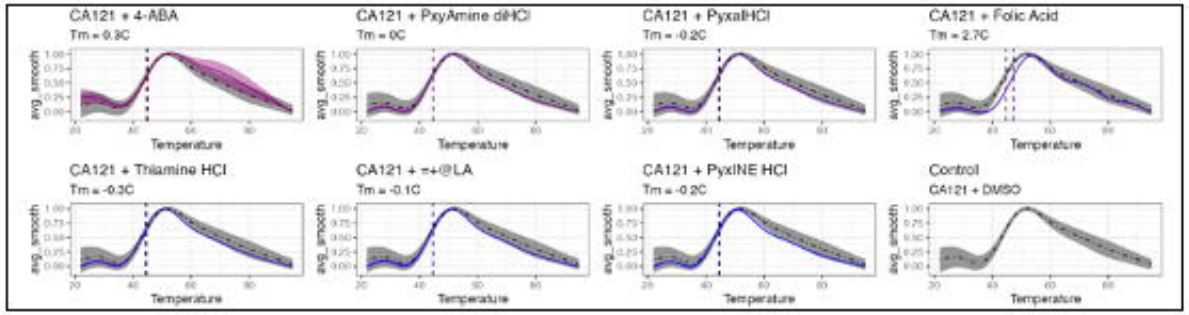
CA121 + 4-ABA
CA121 + PxyAmine dHCl
CA121 + PyxalHCl
CA121 + Folic Acid
CA121 + Thiamine HCl
CA121 + ++@LA
CA121 + PyxINE HCl
Control
CA121 + DMSO
Temperature

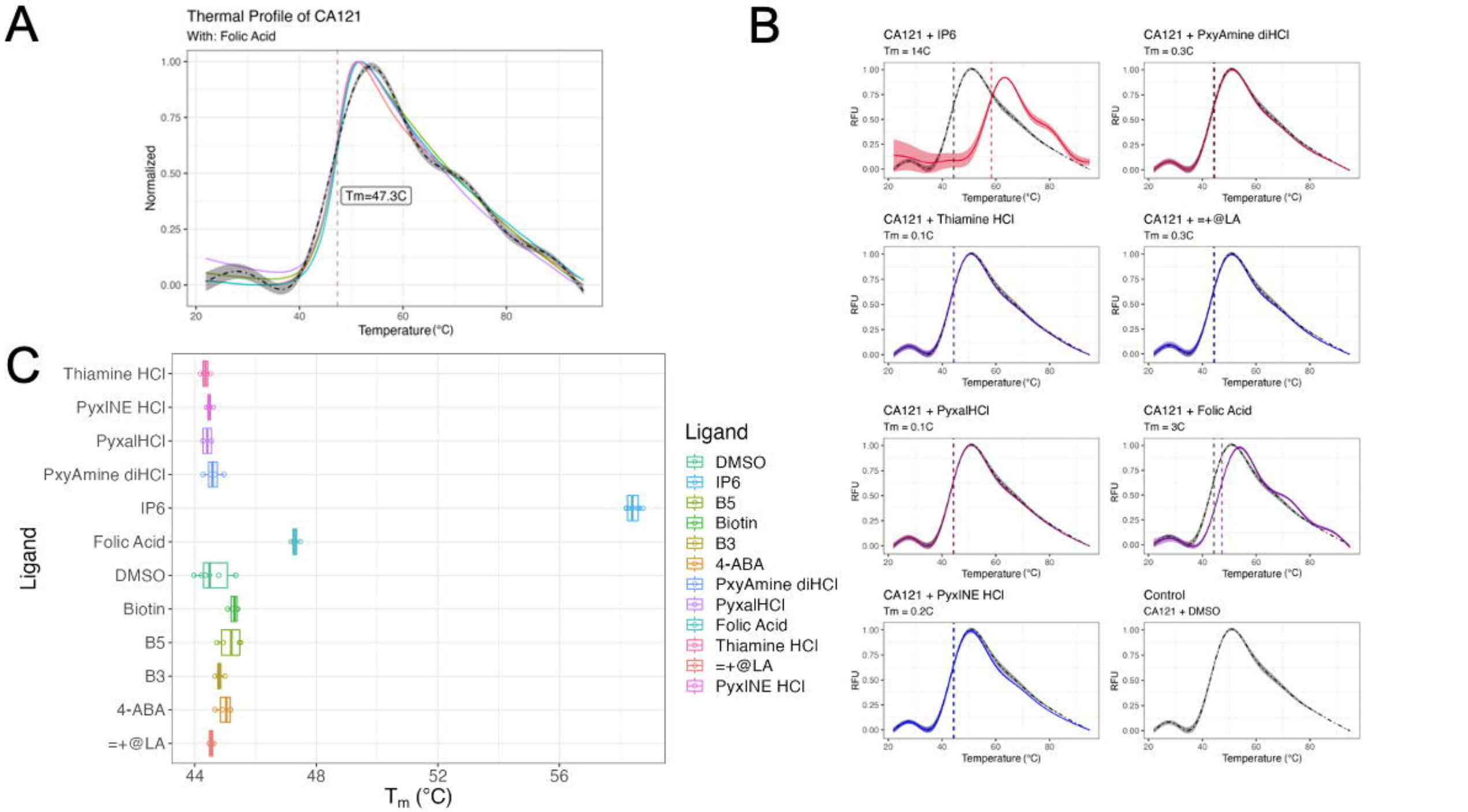
A
Thermal Profile of CA121
With: Folic Acid
Normalized
Tm=47.3C
Temperature (°C)
B
CA121 + IP6
Tm = 14C
CA121 + PxyAmine diHCl
Tm = 0.3C
CA121 + Thiamine HCl
Tm = 0.1C
CA121 + =+@LA
Tm = 0.3C
CA121 + PyxalHCl
Tm = 0.1C
CA121 + Folic Acid
Tm = 3C
CA121 + PyxINE HCl
Tm = 0.2C
Control
CA121 + DMSO
RFU
Temperature (°C)
C
Thiamine HCl
PyxINE HCl
PyxalHCl
PxyAmine diHCl
IP6
Folic Acid
DMSO
Biotin
B5
B3
4-ABA
=+@LA
Ligand
T_m (°C)
Ligand
DMSO
IP6
B5
Biotin
B3
4-ABA
PxyAmine diHCl
PyxalHCl
Folic Acid
Thiamine HCl
=+@LA
PyxINE HCl

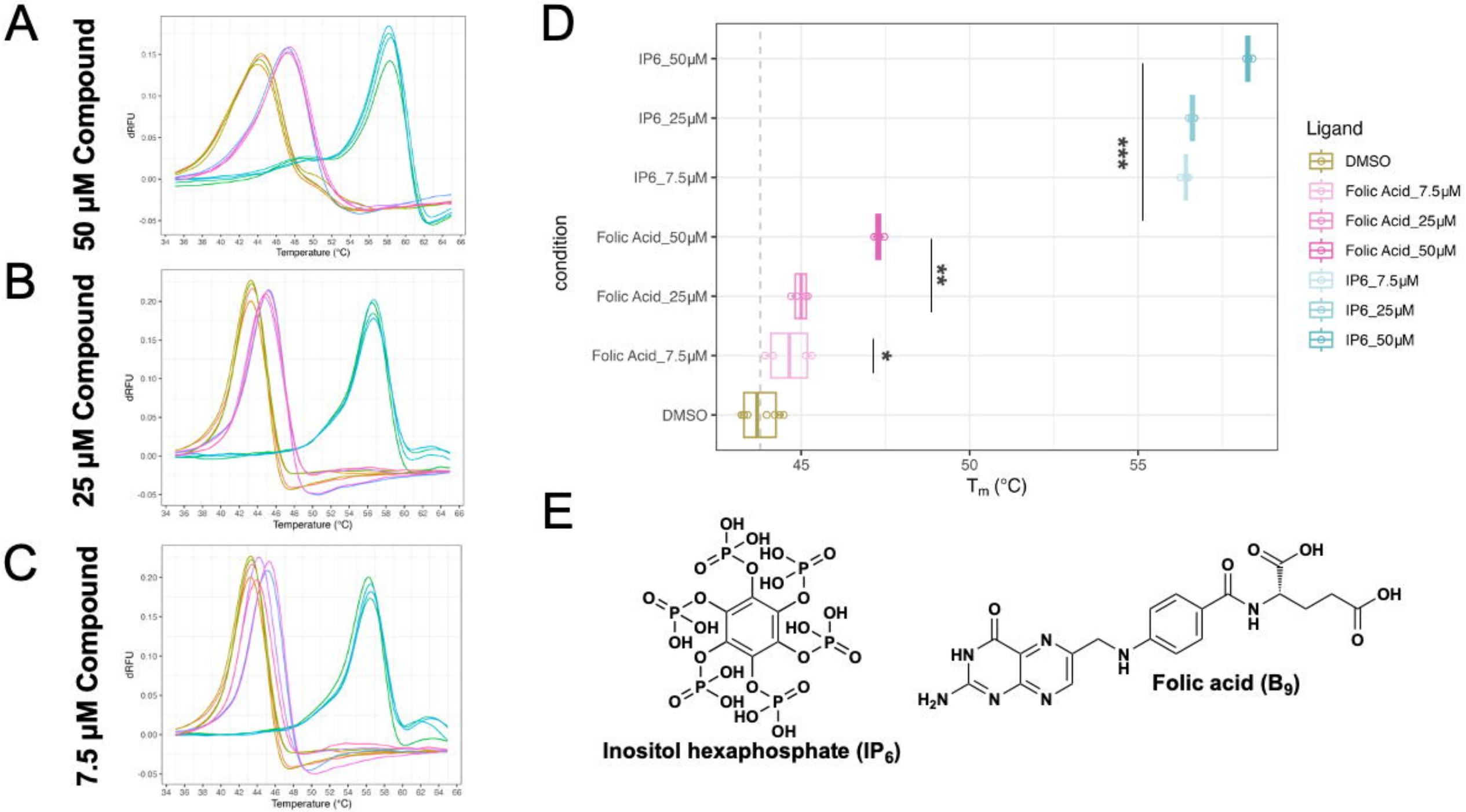
A
50 µM Compound
dRFU
Temperature (°C)
B
25 µM Compound
dRFU
Temperature (°C)
C
7.5 µM Compound
dRFU
Temperature (°C)
D
condition
IP6_50µM
IP6_25µM
IP6_7.5µM
Folic Acid_50µM
Folic Acid_25µM
Folic Acid_7.5µM
DMSO
***
**
*
45
50
55
T_m (°C)
Ligand
DMSO
Folic Acid_7.5µM
Folic Acid_25µM
Folic Acid_50µM
IP6_7.5µM
IP6_25µM
IP6_50µM
E
Inositol hexaphosphate (IP_6)
Folic acid (B_9)

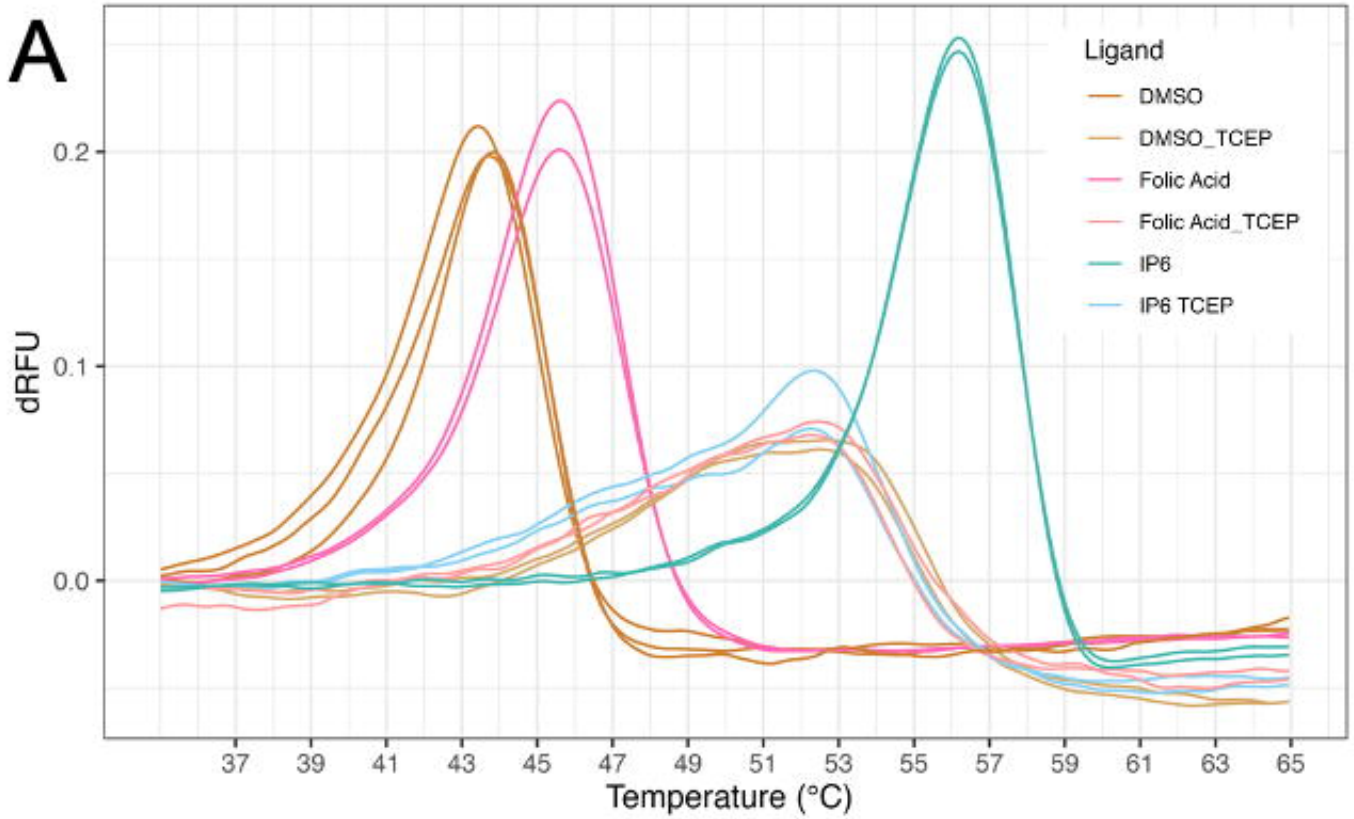
A
Ligand
DMSO
DMSO_TCEP
Folic Acid
Folic Acid_TCEP
IP6
IP6 TCEP
dRFU
0.2
0.1
0.0
37
39
41
43
45
47
49
51
53
55
57
59
61
63
65
Temperature (°C)

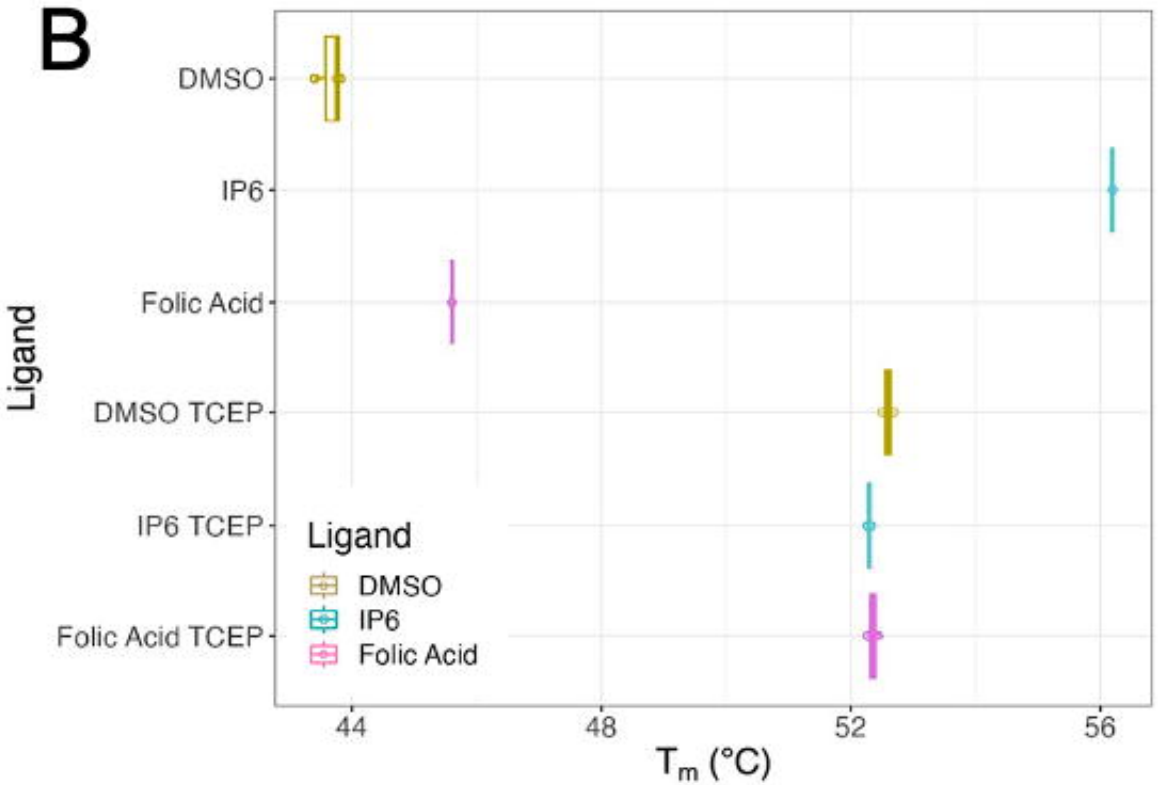
B
DMSO
IP6
Folic Acid
DMSO TCEP
IP6 TCEP
Folic Acid TCEP
Ligand
Ligand
DMSO
IP6
Folic Acid
44
48
52
56
T_m (°C)

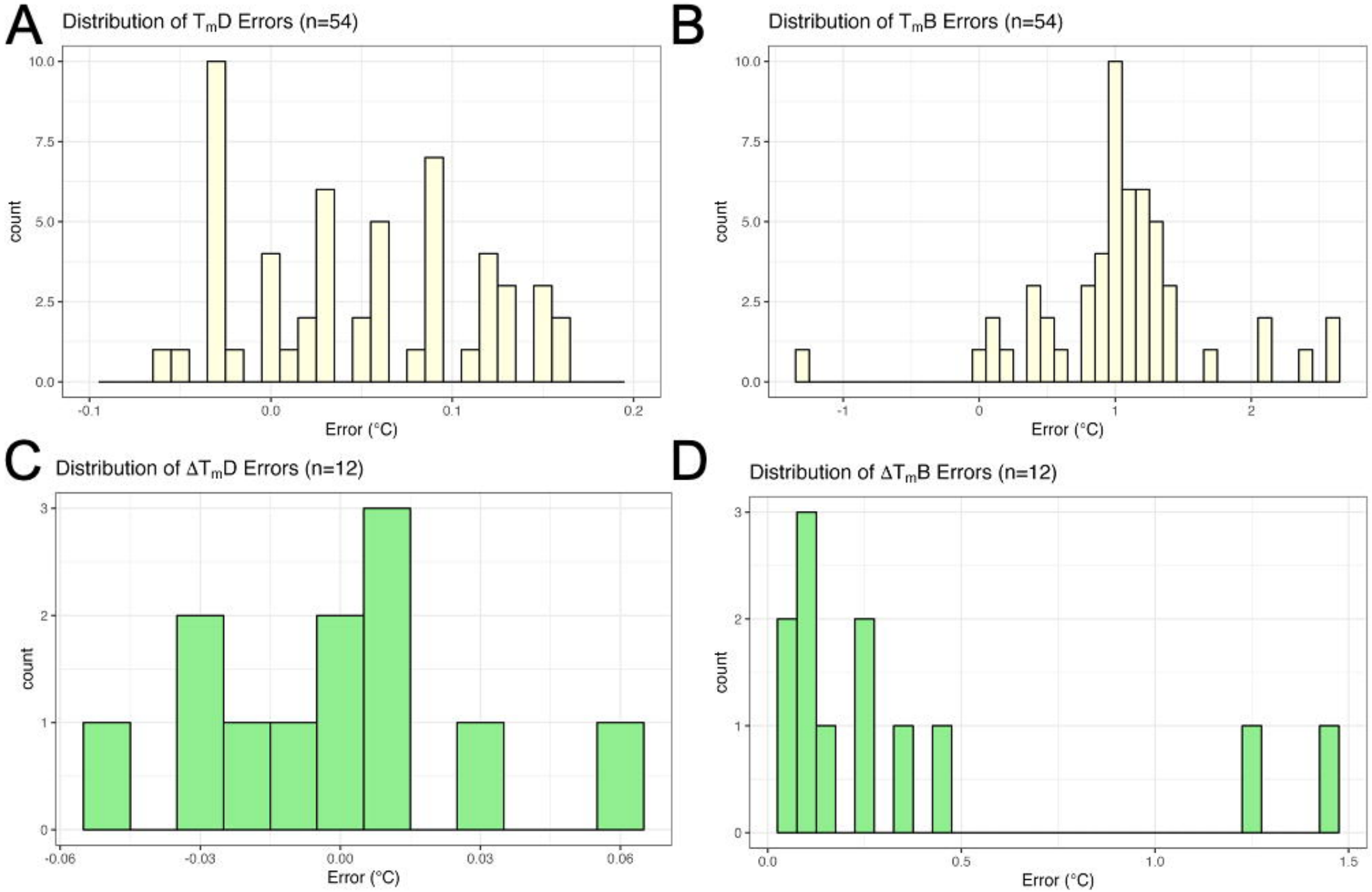
A
Distribution of T_mD Errors (n=54)
count
Error (°C)
B
Distribution of T_mB Errors (n=54)
count
Error (°C)
C
Distribution of ΔT_mD Errors (n=12)
count
Error (°C)
D
Distribution of ΔT_mB Errors (n=12)
count
Error (°C)